JOURNAL OF NATURAL PRODUCTS

Article

pubs.acs.org/jnp

Detailed Analysis of (−)-Palmyrolide A and Some Synthetic Derivatives as Voltage-Gated Sodium Channel Antagonists

Suneet Mehrotra,[†,‡] Brendan M. Duggan,[§,‡] Rodolfo Tello-Aburto,[⊥,∥] Tara D. Newar,[⊥] William H. Gerwick,[§] Thomas F. Murray,[†] and William A. Maio*[,⊥]

[†]Department of Pharmacology, Creighton University School of Medicine, Omaha, Nebraska 68178, United States

[§]Center for Marine Biotechnology and Biomedicine, Scripps Institution of Oceanography and Skaggs School of Pharmacy and Pharmaceutical Sciences, University of California, San Diego, La Jolla, California 92037, United States

[⊥]Department of Chemistry and Biochemistry, New Mexico State University, Las Cruces, New Mexico 88003, United States

Supporting Information

ABSTRACT: A small library of synthetic (−)-palmyrolide A diastereomers, analogues, and acyclic precursors have been examined with respect to their interaction with voltage-gated sodium channels (VGSCs). Toward this goal, the ability of (−)-palmyrolide A and analogues to antagonize veratridine-stimulated Na^+ influx in primary cultures of mouse cerebrocortical neurons was assessed. We found that synthetic (−)-palmyrolide A and its enantiomer functioned as VGSC antagonists to block veratridine-induced sodium influx. A detailed NMR and computational analysis of four diastereomers revealed that none had the same combination of shape and electrostatic potential as exhibited by natural (−)-palmyrolide A. These data indicate that the relative configuration about the *tert*-butyl and methyl substituents appears to be a prerequisite for biological function. Additional testing revealed that the enamide double bond was not necessary for blocking veratridine-induced sodium influx, whereas the acyclic analogues and other macrolide diastereomers tested were inactive as inhibitors of VGSCs, suggesting that the intact macrolide was required.

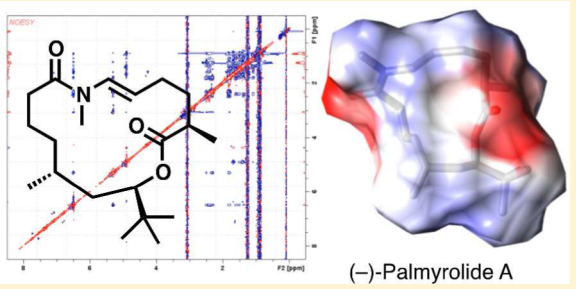

Marine cyanobacteria continue to be an exciting resource for the discovery of novel secondary metabolites that not only possess unique structural features and interesting biological activity but also serve as inspiration for a prodigious number of modern chemotherapies. Recently, as part of a drug discovery screening effort, (−)-palmyrolide A (**1**, Figure 1) was isolated as a neuroactive constituent of a cyanobacterial assemblage collected at Palmyra Atoll in the Central Pacific Ocean.[1] Initial biological studies revealed **1** to significantly suppress calcium ion influx in murine cerebrocortical neurons (IC_{50} = 2.1 μM) and to exhibit potent sodium ion channel blocking activity in Neuro-2a cells (IC_{50} = 5.2 μM) with no appreciable cytotoxicity when screened against human lung adenocarcinoma cells.[1]

Palmyrolide A is a 15-membered macrolide possessing two unique structural elements: a rare *tert*-butyl moiety and a *trans*-*N*-methyl enamide. At present, there have been only a few reports of isolated natural products that contain a sterically encumbered *tert*-butyl group proximal to a lactone ester: the structurally related laingolide series[2] and (−)-apratoxin A.[3] Enamide-containing macrolides are also uncommon in the natural product literature, but both *cis* and *trans* alkenes are documented to exist either endocyclic or exocyclic.[4] Also of note, several natural product families possess the enamide functional group as a side chain or acyclic feature rather than part of a macrolide.[5]

The atom connectivity of palmyrolide A was initially determined by detailed NMR studies;[1] however, as a result of the increased hydrolytic stability imparted to the lactone due to the neighboring *tert*-butyl group, it was difficult to degrade the macrolide into smaller fragments that would be useful in determining its absolute configuration. While exhaustive degradation did allow the C-14 stereocenter to be assigned as *R*, application of the Murata *J*-based configurational analysis directly on the 15-membered macrocycle in conjunction with NOE correlations was necessary to assign the relative relationship between the C-5 methyl and C-7 *tert*-butyl as *syn*.[1] This assignment was subsequently revised as *anti* through a total synthesis campaign in which four diastereo combinations: two bearing the natural C-14(*R*) methyl group (**1**, **8**) and two with the non-natural C-14(S) geometry (**2**, **7**).

With several diastereomers on hand from our first total synthesis campaign (**1**, **3**, **4**, **7**, **8**, Figure 1), one new diastereomer (**2**), two saturated compounds derived via enamide hydrogenation (**5**, **6**), and several acyclic precursors (**9**−**12**), we sought to determine the ability of these non-natural synthetic derivatives to antagonize veratridine-stimulated Na^+ influx in primary cultures of mouse cerebrocortical

Received: August 13, 2014
Published: October 24, 2014

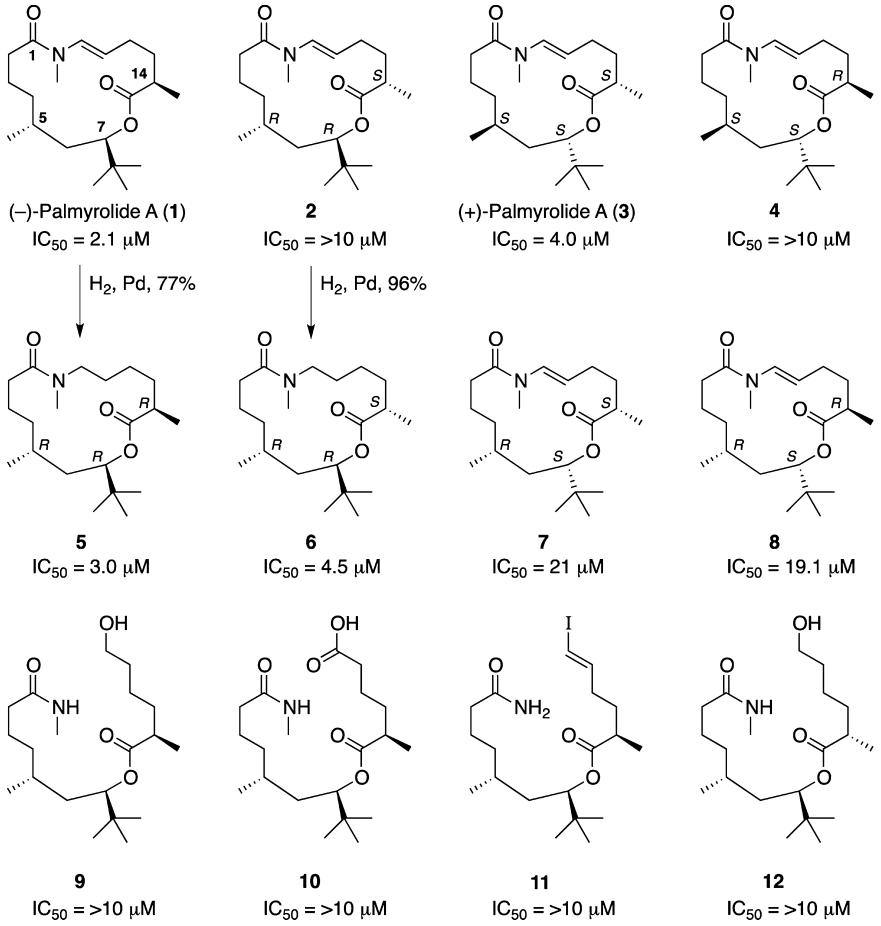

Figure 1. Palmyrolide macrolide diastereomers and related compounds.

neurons compared to natural palmyrolide A. In conjunction with this study and to better understand how structure relates to biological function for these palmyrolide analogues, an exhaustive NMR and computational analysis was conducted on four diastereo combinations: two bearing the natural C-14(*R*) methyl group (**1**, **8**) and two with the non-natural C-14(*S*) geometry (**2**, **7**).

RESULTS AND DISCUSSION

Synthetic Studies. Compounds **1**–**4**, **7**, **8**, and **11** were synthesized following our previously reported synthetic routes.[6] Saturated derivatives **5** and **6**, unique to this work, were synthesized via the hydrogenation of diastereomers **1** and **2**, respectively. Palmyrolide alcohol (**9**) and acid (**10**) were prepared exploiting the known acid-catalyzed ring opening of **1**,[1] followed by treating the resultant aldehyde with either $NaBH_4$ (for **9**) or $NaClO_2$ (for **10**). Alcohol **12** could be accessed in a similar manner from 14-*epi*-palmyrolide (**2**).

Antagonism of Veratridine-Induced Na^+ Influx. In order to detect an interaction of (−)-palmyrolide A and its analogues with voltage-gated sodium channels (VGSCs), we examined the ability of these compounds to antagonize veratridine-stimulated Na^+ influx in murine primary cerebrocortical neurons. We previously demonstrated that veratridine is a partial agonist at neurotoxin site 2 on the VGSC α subunit.[8] Murine cerebrocortical neurons were loaded with the Na^+-binding benzofuran isophthalate (SBFI), and the ability of palmyrolide analogues to block veratridine-induced elevation of neuronal $[Na^+]_i$ was determined.

Table 1. Calculated IC_{50} Values with 95% Confidence Intervals (CI) for (−)-Palmyrolide A and Each of the 11 Analogues Tested[a]

palmyrolide and derivatives	IC_{50} (μM)[b]	95% CI (μM)
1	2.1	1.2–3.1
5	3.0	1.9–4.8
3	4.0	2.7–6.0
6	4.5	2.1–9.3
8	19.1	4.6–78.5
7	21	5.1–86.3
2	>10	
4	>10	
9	>10	
10	>10	
11	>10	
12	>10	

[a]Antagonism of veratridine-stimulated Na^+ influx in murine cerebrocortical neurons. [b]Values represent mean ± SEM of 2–5 experiments each performed with 2–10 replicates.

Naturally occurring (−)-palmyrolide A is a neuroactive macrolide that was previously shown to block veratridine-induced sodium influx in Neuro-2a cells (IC_{50} = 5.2 μM)[1] and to display significant inhibition of Ca^{2+} oscillation in murine cerebrocortical neurons, with an IC_{50} value of 3.70 μM (2.29–5.98 μM, 95% CI).[1] We have confirmed and extended these original findings by demonstrating that synthetic (−)-palmyrolide A (**1**, Figures 2A and 3A) and its enantiomer (**3**, Figures

dx.doi.org/10.1021/np500644k | J. Nat. Prod. 2014, 77, 2553–2560

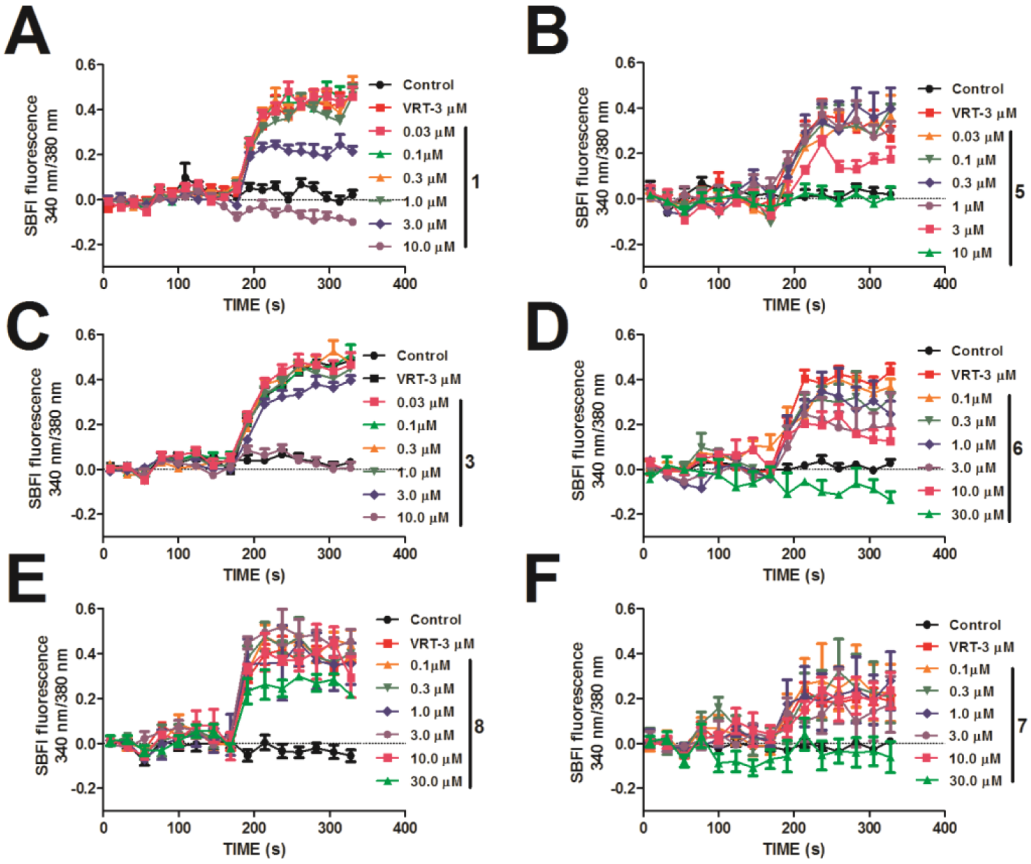

Figure 2. Time-response analysis of (−)-palmyrolide A and active analogues. Sodium influx was monitored with SBFI (340/380) responses to veratridine in the absence and presence of (−)-palmyrolide A and its analogues. The compounds shown are (A) (−)-palmyrolide A (**1**); (B) 17,18-dihydropalmyrolide A (**5**); (C) (+)-palmyrolide A (**3**); (D) 17,18-dihydro-14-*epi*-palmyrolide A (**6**); (E) [C-5(*R*),C-7(*S*),C-14(*R*)]-palmyrolide (**8**); and (F) [C-5(*R*),C-7(*S*),C-14(*S*)]-palmyrolide (**7**). Data shown are from a representative experiment performed in 2 or 3 replicates for each concentration. In total 4−7 experiments were performed for each compound (A−F).

2C and 3C) produced concentration-dependent antagonism of veratridine-induced increase in neuronal $[Na^+]_i$. The concentration−response curves for these compounds were best fit by a three-parameter logistic equation. This analysis yielded an IC_{50} value (95% confidence interval) of 2.1 μM (1.2−3.1, 95% CI), which was in good agreement with the IC_{50} value reported earlier for natural (−)-palmyrolide A.[1] We found that (−)-palmyrolide A (**1**) and macrolide analogues **5** and **3** were approximately 3−9-fold more potent than the other analogues tested (Figures 2A−C and 3A−C). The observation that saturated congener **5** showed a comparable IC_{50} to synthetic (−)-palmyrolide A suggests that the enamide double bond is not essential for activity. It is moreover noteworthy that acyclic analogues of (−)-palmyrolide A with the natural absolute configuration were inactive as blockers of veratridine-stimulated Na^+ influx. These data indicate that the three-dimensional molecular shape of (−)-palmyrolide A was crucial for the interaction with VGSCs.

In order to support these observations and to better understand how structure relates to biological function, an exhaustive NMR and computational analysis was next conducted on **1** and three diastereomers (i.e., **2**, **7**, and **8**). Saturated derivatives **5** and **6** exist as a mixture of rotational isomers and precluded precise NMR assignments from being made.

NMR and Computational Studies for Palmyrolide A and Diastereomers. Chemical shift assignments of (−)-palmyrolide A (**1**) and synthetic diastereomers **2**, **7**, and **8** were made using DQF-COSY, HSQC, HMBC, and H2BC spectra. The chemical shifts of these four diastereomeric compounds follow the same general trends but differ slightly, indicating that the conformations of the macrolide ring are different. For example, in each diastereomer a different methylene group exhibited degenerate chemical shifts for its two protons. Stereospecific assignments were made for most of the prochiral atoms that possessed nondegenerate shifts. The NOESY spectra provided 74 nonredundant distance restraints for **1**, 83 for **2**, 84 for **7**, and 77 for **8**. Several torsion restraints were derived from $^1H-^1H$ coupling in the ^1H NMR spectra and from the heteronuclear couplings measured by the HETLOC experiments (see Supporting Information for all restraints). Applying the distance and torsion restraints during simulated annealing calculations produced fairly well-defined ensembles of structures. The violation energies were low with no distance violation greater than 0.19 Å. Table 2 summarizes the inputs and results of the structure calculations.

To test the specificity of the restraints and their ability to discriminate between the four diastereomers, restrained simulated annealing calculations were performed for all 16 combinations of starting structure and restraint set. If the restraints correctly discriminated between conformations, then the correct combination should have the least restraint violations and the lowest energy. For all four structures we found the best restraint set for each starting structure was the

dx.doi.org/10.1021/np500644k | *J. Nat. Prod.* 2014, 77, 2553−2560

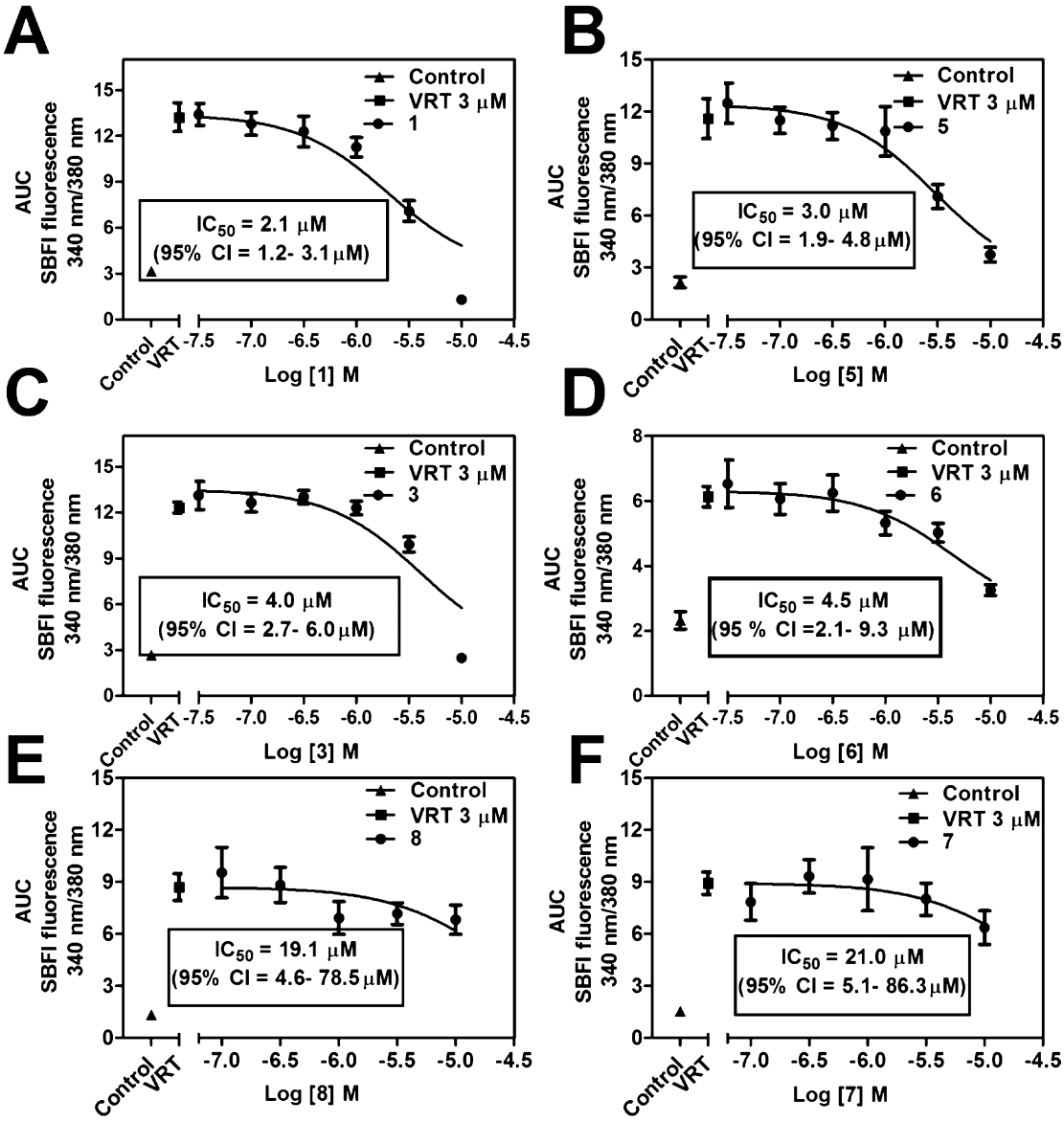

Figure 3. Nonlinear regression analysis of concentration−response data for active analogues of (−)-palmyrolide A. A three-parameter logistic fit of the palmyrolide A analogue inhibition of the response to veratridine is shown for each active compound. The compounds shown are (A) (−)-palmyrolide A (**1**); (B) 17,18-dihydropalmyrolide A (**5**); (C) (+)-palmyrolide A (**3**); (D) 17,18-dihydro-14-*epi*-palmyrolide A (**6**); (E) [C-5(*R*),C-7(*S*),C-14(*R*)]-palmyrolide (**8**); and (F) [C-5(*R*),C-7(*S*),C-14(*S*)]-palmyrolide (**7**). Data points shown represent the mean ± SEM of 2−5 experiments performed with 2−10 replicates each (A−F).

Table 2. Structure Calculation Statistics

	1 [C-5(*R*), C-7(*R*), C-14(*R*)]	**2** [C-5(*R*), C-7(*R*), C-14(*S*)]	**7** [C-5(*R*), C-7(*S*), C-14(*S*)]	**8** [C-5(*R*), C-7(*S*), C-14(*R*)]
no. of stereoassignments[a]	4/8	10/12	8/10	6/10
no. of distance restraints	74	83	84	77
no. of torsion restraints	5	5	1	2
no. of structures selected[b]	16	16	17	16
Amber energy (kcal mol^{-1})[c]	36.55 (4.08)	33.67 (2.34)	29.30 (2.09)	27.51 (2.02)
violation energy (kcal mol^{-1})[d]	0.75 (0.39)	0.56 (0.83)	0.07 (0.04)	0.00 (0.00)
rmsd (Å)[e]	0.747	0.496	0.518	0.071

[a]Number of diastereotopic hydrogens for which stereospecific assignments were obtained, and total number of protons with nondegenerate chemical shifts. [b]Number of structures selected based on restraint violations of the 20 calculated. [c]Average Amber energy of the selected ensemble with standard deviation in parentheses. [d]Average violation energy of the selected ensemble with standard deviation in parentheses. [e]rmsd of atoms C-1−C-7, O-12, C-13−C-18, and N-19.

correct one, namely, the restraints derived from NMR spectra of that compound (Table 3). This confirms that the restraint sets were able to correctly discriminate between the diastereomers.

dx.doi.org/10.1021/np500644k | *J. Nat. Prod.* 2014, 77, 2553−2560

Table 3. Specificity of Restraints

starting structure	**1** [C-5(*R*), C-7(*R*), C-14(*R*)] restraints[a]			**2** [C-5(*R*), C-7(*R*), C-14(*S*)] restraints			**7** [C-5(*R*), C-7(*S*), C-14(*S*)] restraints			**8** [C-5(*R*), C-7(*S*), C-14(*R*)] restraints		
1	*16*	*36.55*	*0.75*	15	108.03	47.06	12	53.05	2.89	17	78.83	14.17
2	13	48.25	14.23	*16*	*33.67*	*0.56*	13	43.77	2.50	15	42.06	4.19
7	18	48.21	14.43	14	33.18	0.53	*17*	*29.30*	*0.07*	14	34.56	0.99
8	17	48.44	14.62	14	32.18	1.51	19	31.82	0.04	*16*	*27.51*	*0.00*

[a]The three numbers reported for each combination of starting structure and restraint set are number of selected structures, average Amber energy, and average violation energy. The italic cells indicate the best set of restraints for each starting structure, with respect to Amber energy and violation energy, and also correspond to the correct pairing.

The four ensembles generally have the same overall conformation, with the major differences being due to the orientations of the substitutents. All four diastereomers have a *cisoid* configuration of the *N*-methyl group (N-CH_3) and the adjacent carbonyl despite the starting structures having a *transoid* configuration. Examining the trajectories reveals that the configuration converts early in the simulated annealing as the restraints take effect. The driving force in these simulations appears to be NOEs between H-18 and the H-2 methylene group.

To quantify differences between the ensembles, we calculated root-mean-square deviations (rmsd's) between the representative structures of each ensemble (Table 4). The rmsd's were calculated using the differences in the positions of the carbon, nitrogen, and oxygen atoms of the macrolide ring after aligning the structures to minimize these differences. Representative structures were selected as the structure having the smallest rmsd among all other structures in its ensemble. The rmsd's between all four representative structures were similar (Table 4), with **2** having the lowest values overall, suggesting that this ensemble is the most "central" in comparison to the other diastereomers.

Table 4. RMSDs between Representative Structures

	1 [C-5(*R*), C-7(*R*), C-14(*R*)]	**2** [C-5(*R*), C-7(*R*), C-14(*S*)]	**8** [C-5(*R*), C-7(*S*), C-14(*R*)]	**7** [C-5(*R*), C-7(*S*), C-14(*S*)]
(−)-palmyrolide A (**1**)		1.443	1.341	1.750
2	1.443		1.233	1.320
8	1.341	1.233		1.604
7	1.750	1.320	1.604	
sum[a]	4.534	3.996	4.178	4.674

[a]The final row is the sum of the three rmsd's above, a measure of the total difference from the other structures.

Visual inspection of the ensembles shows that the macrolide ring is relatively flat, but the orientation of the *tert*-butyl and methyl groups alters the global shape (Figure 4). In **1** the *tert*-butyl and methyl groups lie close to the plane of the ring, but in **7** the *tert*-butyl group projects almost perpendicular to the plane of the ring, and in **8** the two methyl groups project in opposite directions above and below the ring. Examining the surface electrostatic potential of the representative structures (Figure 5) we find that **8** is the most similar to the active compound **1**. However, the C-14 methyl group in **1** projects to the side, whereas in **8** it is situated above the macrolide ring. Taken together, these differences between diastereomers may account, at least in part, for the observed differences in biological activity. In addition, due to the highly flexible nature of the macrolide, as evidenced through computational modeling, the minimized ligand ensembles reported here may not necessarily reflect the structure these molecules adopt when bound to their molecular target. Further consideration and investigations into structure−activity relationships are ongoing and will be reported in due course.

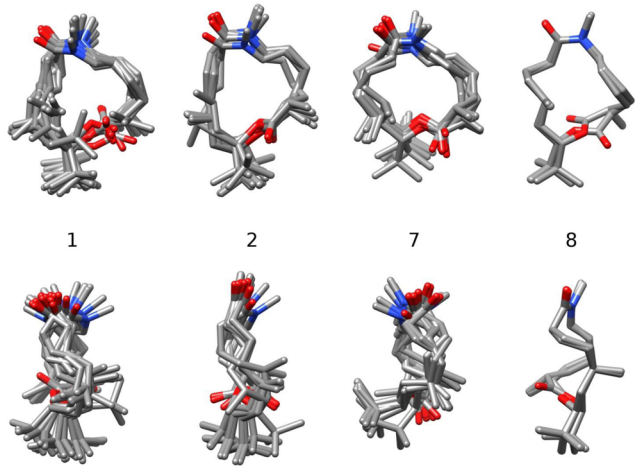

Figure 4. NMR restraint-derived ensembles. The lower row shows the ensembles rotated by 90° about the vertical axis.

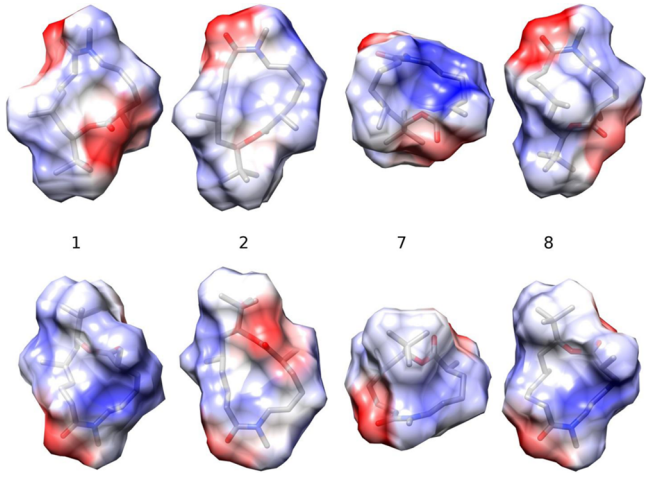

Figure 5. Surface electrostatic potential of the representative structures of each ensemble. The four structures in the top row are shown in a similar orientation to Figure 4. In the lower row the structures have been rotated 180° about the horizontal axis to show the rear face. The electrostatic potential ranges from red (−2 kcal/mol·e) through white (0) to blue (+2 kcal/mol·e).

dx.doi.org/10.1021/np500644k | *J. Nat. Prod.* 2014, 77, 2553−2560

CONCLUSION

These findings suggest that both synthetic (−)-palmyrolide A and its enantiomer function with equal potency as VGSC antagonists to block veratridine-induced sodium influx. With regard to identification of the pharmacophore of this natural product, it appears that the intact macrolide is required since acyclic versions were inactive as inhibitors of VGSCs. Moreover, analogues lacking the enamide double bond were of high potency in this assay, and thus this functionality appears unnecessary for blocking VGSCs. Finally, using detailed NMR and computational approaches with the natural product and three diastereomeric analogues, it was found that the C-5−C-7 *anti*/C-7−C14 *syn* arrangement of stereocenters produces a unique combination of three-dimensional shape and electrostatic potential that is responsible for the potent biological activity of the natural product. In an effort to understand the similar biological activity found for the natural stereoisomer and its enantiomer, continued investigations in this area will focus on uncovering the specific molecular target and associated binding site, which may also assist in future analogue development of novel sodium channel blocking analgesics derived from palmyrolide A.

EXPERIMENTAL SECTION

General Experimental Procedures. Unless otherwise noted, reactions were performed in flame-dried glassware under an atmosphere of dry nitrogen. Reaction solvents (CH_2Cl_2, THF, and Et_2O) were purified before use in a solvent purification system under a flow of dry nitrogen. All other solvents and reagents were purchased from commercial suppliers and used as received, unless otherwise specified. Thin-layer chromatography (TLC) was performed using plates precoated with silica gel 60 Å F-254 (250 μm) and visualized by UV light, $KMnO_4$, or anisaldehyde stains, followed by heating. Silica gel (particle size 40−63 μm) was used for flash chromatography. Optical rotation values were recorded using a Jasco P-2000 polarimeter. IR samples were prepared by evaporation from $CHCl_3$ or CH_2Cl_2 on NaCl plates and run on a PerkinElmer Spectrum One FT-IR spectrometer. For the synthetic studies, ^{1}H and ^{13}C NMR spectra were recorded at 300 and 75 MHz (Oxford magnet with a Varian 300 console), at 400 and 100 MHz (Oxford magnet with a Varian Unity 400 console), and at 600 and 150 MHz (Magnex magnet with a Bruker Avance III 600 console), respectively, and are reported relative to residual solvent peak (δ_H 7.26 and δ_C 77.0 for ^{1}H and ^{13}C in $CDCl_3$). High-resolution mass spectra were obtained using positive electrospray ionization on a Bruker 12 T APEX-Qe FTICR-MS with an Apollo II ion source at the COSMIC Laboratory facility at Old Dominion University, VA.

Synthetic Studies. *14-epi-Palmyrolide A (**2**).* To a solution of (*S*,*E*)-6-iodo-2-methylhex-5-enoic acid (0.096 g, 0.37 mmol) in THF (3.7 mL) was added diisopropylethylamine (0.100 mL, 0.60 mmol) followed by the Yamaguchi reagent (0.071 mL, 0.45 mmol). The mixture was allowed to stir at room temperature for 3 h before being concentrated *in vacuo*. The resultant mixed anhydride was dissolved in toluene (7.4 mL) and then added, via cannula, to a flask containing (5*R*,7*R*)-7-hydroxy-5,8,8-trimethylnonanamide (0.051 g, 0.23 mmol) and DMAP (0.046 g, 0.37 mmol). After stirring at room temperature (rt) for 12 h, the reaction mixture was diluted with CH_2Cl_2, washed with a saturated aqueous solution of $NaHCO_3$, dried over $MgSO_4$, and concentrated. Purification via flash column chromatography (1:1 hexanes/EtOAc) afforded 0.088 g (81%) of the coupled product as a colorless oil: $[\alpha]_D^{22.5}$ +13.3 (*c* 1.98, $CHCl_3$); IR (neat, thin film) ν 3429, 3351, 3203, 2962, 2934, 2868, 1725, 1665, 1607, 1461, 1380, 1366, 1259, 1181, 1119, 1067, 957, 935 cm^{-1}; ^{1}H NMR (300 MHz, $CDCl_3$) δ 6.49 (dt, *J* = 7.2, 14.4 Hz, 1 H), 6.02 (d, *J* = 14.4 Hz, 1H), 5.88 (bs, 1 H), 5.46 (bs, 1 H), 4.79 (dd, *J* = 4.5, 6.3 Hz, 1 H), 2.45 (sextet, *J* = 6.9 Hz, 1 H), 2.23−2.15 (m, 2 H), 2.12−2.05 (m, 2 H), 1.86−1.69 (m, 2 H), 1.61−1.25 (m, 6 H), 1.17 (d, *J* = 7.2 Hz, 3 H), 1.11−0.99 (m, 1 H), 0.91−0.87 (overlapping doublet/singlet, 12 H); ^{13}C NMR (75 MHz, $CDCl_3$) δ 176.5, 175.8, 145.6, 79.0, 75.5, 39.3, 37.7, 35.7, 34.79, 34.77, 33.9, 32.3, 29.2, 26.1, 22.8, 21.1, 17.5; HRESIMS *m*/*z* 474.1471 $[M + Na]^+$ (calcd for $C_{19}H_{34}INO_3Na$, 474.1476).

To the coupled product (0.088 g, 0.19 mmol) in THF (19.0 mL) was added CuI (0.005 g, 0.03 mmol) and Cs_2CO_3 (0.100 g, 0.30 mmol). The mixture was first degassed using nitrogen (10 min) before *N*,*N*′-dimethylethylenediamine (0.050 mL, 0.46 mmol) was added. The rubber septum was quickly replaced with a glass stopper, and the reaction mixture heated to 60 °C for 19 h. After cooling to rt, the reaction mixture was diluted with EtOAc, filtered through a short plug of silica, and concentrated. The crude product was purified via flash column chromatography (8:2 → 7:3 → 1:1 hexanes/EtOAc) to yield the *N*-H enamide intermediate (0.022 g), which was immediately dissolved in THF (0.7 mL) and cooled to 0 °C. To this was added NaH (0.014 g, 0.34 mmol, 60% in mineral oil) in a single portion. The reaction mixture was allowed to stir for 20 min before MeI (0.100 mL) was added dropwise, followed by removal of the ice water bath. After being allowed to stir at rt for 20 min, the reaction mixture was again cooled to 0 °C before being quenched with H_2O, extracted using EtOAc, dried over $MgSO_4$, and concentrated. The crude product was purified via flash column chromatography (9:1 hexanes/EtOAc) to yield 14-*epi*-palmyrolide A (0.016 g, 25% over two steps) as a colorless oil: $[\alpha]_D^{24.5}$ −11.4 (*c* 0.58, $CHCl_3$); IR (neat, thin film) ν 2959, 2927, 2873, 1728, 1675, 1646, 1466, 1413, 1384, 1366, 1333, 1298, 1240, 1205, 1193, 1171,1121, 933 cm^{-1}; ^{1}H NMR (400 MHz, $CDCl_3$) δ 6.63 (d, *J* = 13.6 Hz, 1 H), 4.92 (ddd, *J* = 5.2, 8.8, 13.6 Hz, 1 H), 4.85 (dd, *J* = 2.0, 9.6, 1 H), 3.05 (s, 3 H), 2.60−2.42 (m, 3 H), 2.32 (dt, *J* = 7.2, 13.6 Hz, 1 H), 2.24−2.17 (m, 1 H), 2.03−1.95 (m, 1 H), 1.84−1.74 (m, 1 H), 1.68−1.54 (m, 2 H), 1.49−1.30 (m, 4 H), 1.26 (d, *J* = 7.2 Hz, 3 H), 1.03−0.93 (m, 1 H), 0.89 (d, *J* = 6.4 Hz, 3 H), 0.86 (s, 9 H); ^{13}C NMR (100 MHz, $CDCl_3$) δ 175.4, 172.8, 129.8, 110.2, 76.5, 37.2, 36.6, 35.4, 34.3, 33.6, 31.0, 29.8, 29.5, 27.3, 25.9, 24.9, 20.0, 19.2; HRESIMS *m*/*z* 360.2504 $[M + Na]^+$ (calcd for $C_{20}H_{35}NO_3Na$, 360.2509).

*17,18-Dihydropalmyrolide A (**5**).* To a solution of (−)-palmyrolideA (0.008 g, 0.022 mmol) in anhydrous MeOH (1 mL) was added 10% palladium on carbon (0.005 g). The atmosphere in the flask was replaced with hydrogen, and the reaction mixture was allowed to stir at rt for 18 h before being filtered through a short plug of silica. After rinsing several times with ether, the filtrate was concentrated and purified via column chromatography (8:2 hexanes/EtOAc) to afford compound **5** (0.006 g, 77%) as a mixture of rotational isomers (~2:1 ratio): $[\alpha]_D^{23}$ +35.6 (*c* 0.48, $CHCl_3$); IR (neat, thin film) ν 2954, 2931, 2871, 1720, 1651, 1269, 1250, 1073 cm^{-1}; ^{1}H NMR (300 MHz, $CDCl_3$, mixture of rotational isomers with mostly overlapping peaks, making the assignment of major and minor components difficult) δ (major isomer) 4.82 (d, *J* = 10.0 Hz, 1 H), 3.30 (t, *J* = 5.0 Hz, 1 H), 2.98 (s, 3 H), 2.53−2.65 (m, 2 H), 2.21−2.33 (m, 2 H), 1.21−1.73 (m, 14 H), 1.18 (d, *J* = 6.9 Hz, 3 H), 0.94 (d, *J* = 5.9 Hz, 3 H), 0.86 (s, 9 H), (minor isomer, partial) 4.92 (d, *J* = 10.8 Hz, 0.6 H), 2.89 (s, 1.5 H), 0.91 (d, *J* = 6.1 Hz, 1.5 H); ^{13}C NMR (75 MHz, $CDCl_3$, mixture of rotational isomers) δ 175.5, 174.8, 173.5, 77.8, 77.2, 48.9, 46.3, 40.4, 40.0, 38.3, 37.2, 35.2, 35.0, 33.6, 33.2, 32.98, 32.96, 31.2, 39.7, 27.9, 27.6, 27.0, 26.0, 25.9, 25.4, 23.5, 23.2, 22.2, 20.4, 20.1, 18.0, 16.5; HRESIMS *m*/*z* 362.2660 $[M + Na]^+$ (calcd for $C_{20}H_{37}NO_3Na$, 362.2665).

*17, 18-Dihydro-14-epi-palmyrolide A (**6**).* Compound **6** was prepared in a similar manner to **5**. The crude product was purified via column chromatography (8:2 hexanes/EtOAc) to afford compound **6** (0.006 g, 96%) as a mixture of rotational isomers (~2:1 ratio): $[\alpha]_D^{23}$ +42.1 (*c* 0.5, $CHCl_3$); IR (neat, thin film) ν 2956, 2930, 2872, 1727, 1647, 1459, 1192, 1156 cm^{-1}; ^{1}H NMR (300 MHz, $CDCl_3$, mixture of rotational isomers with mostly overlapping peaks, making the assignment of major and minor components difficult) δ (major isomer) 4.86 (d, *J* = 10.5 Hz, 1 H), 3.51−3.42 (m, 1 H), 3.23−3.14 (m, 1 Hz), 2.88 (s, 3 H), 2.31−2.48 (m, 2 H), 2.18−2.31 (m, 2 H), 1.97−1.79 (m, 2 H), 1.23−1.66 (m, 15 H), 1.19 (d, *J* = 7.0 Hz, 3 H), 0.92 (d, *J* = 5.8 Hz, 3 H), 0.86 (s, 11 H), (minor isomer, partial) 4.83 (d, *J* = 11.6 Hz, 0.6 H), 2.91 (s, 1 H), 1.15 (d, *J* = 7.2 Hz, 1.5 H),

dx.doi.org/10.1021/np500644k | *J. Nat. Prod.* 2014, 77, 2553−2560

0.96 (d, J = 5.7 Hz, 1.5 H); ^{13}C NMR (75 MHz, $CDCl_3$, mixture of rotational isomers) δ 176.8, 176.6, 173.3, 173.0, 77.2, 49.1, 46.0, 40.6, 40.1, 38.0, 37.3, 35.2, 34.0, 33.9, 33.2, 33.1, 33.0, 31.3, 29.7, 28.9, 27.2, 25.9, 24.8, 23.9, 22.8, 19.9, 19.8, 19.2, 19.1; HRESIMS m/z 362.2659 $[M + Na]^+$ (calcd for $C_{20}H_{37}NO_3Na$, 362.2665).

*Palmyrolide Alcohol (**9**).* To a solution of **1** (0.007 g, 0.021 mmol) in $CHCl_3$ (2 mL) was added a 6 N aqueous HCl solution dropwise until TLC analysis showed complete consumption of the starting material. The reaction mixture was then quenched with a saturated aqueous solution of $NaHCO_3$, followed by extraction using EtOAc. The combined organic layers were dried over $MgSO_4$, filtered, and concentrated. The resultant crude aldehyde was dissolved in anhydrous MeOH (1 mL) and treated with $NaBH_4$ (0.015 g, 0.39 mmol). The reaction mixture was allowed to stir at rt for 1 h before being quenched with H_2O, extracted using EtOAc, dried over $MgSO_4$, filtered, and concentrated. The crude alcohol was purified by column chromatography (100% EtOAc) to afford alcohol **9** (0.006 g, 73% over two steps) as a colorless oil: $[\alpha]_D^{24.3}$ +26.8 (c 0.20, $CHCl_3$); IR (neat, thin film) ν 3296, 2956, 1728, 1651, 1562, 1462, 1366, 1164 cm^{-1}; ^{1}H NMR (300 MHz, $CDCl_3$) δ 6.10 (bs, 1 H), 4.76 (dd, J = 2.2, 9.5 Hz, 1 H), 3.63 (t, J = 6.4 Hz, 2 H), 2.79 (d, J = 4.8 Hz, 3 H), 2.39−2.51 (m, 1 H), 2.00−2.23 (m, 2 H), 1.91 (bs, 1 H), 1.63−1.80 (m, 2 H), 1.22−1.60 (m, 10 H), 1.16 (d, J = 7.0 Hz, 3 H), 0.87 (d, overlapped, 3 H), 0.86 (s, 9 H); ^{13}C NMR (75 MHz, $CDCl_3$) δ 176.8, 174.0, 78.6, 62.5, 40.2, 37.6, 36.2, 34.5, 33.3, 32.5, 28.8, 26.2, 25.9, 25.9, 23.5, 23.0, 20.8, 17.4; HRESIMS m/z 380.2764 $[M + Na]^+$ (calcd for $C_{20}H_{39}NO_4Na$, 380.2771).

*Palmyrolide Acid (**10**).* Approximately 0.3 mL of an oxidant solution prepared via the mixing of $NaClO_2$ (0.060 g) and $NaHPO_4$ (0.040 g) in H_2O (1 mL) was added to a solution of palmyrolide aldehyde (prepared as above, 0.006 g, 0.016 mmol) in *tert*-butanol (0.25 mL) and 2-methyl-2-butene (0.1 mL). The reaction mixture was allowed to stir for 30 min before being quenched with water, extracted with EtOAc, dried over $MgSO_4$, filtered, and concentrated. The crude acid was purified by column chromatography (100% EtOAc) to afford acid **10** (0.002 g, 25%) as a colorless oil: $[\alpha]_D^{23}$ +10.8 (c 0.10, $CHCl_3$); IR (neat, thin film) ν 3306, 2960, 1727, 1633, 1164 cm^{-1}; ^{1}H NMR (300 MHz, $CDCl_3$) δ 6.04 (bs, 1 H), 4.78 (dd, J = 10.2, 1.9 Hz, 1 H), 2.82 (d, J = 4.8 Hz, 3 H), 2.48 (q, J = 6.9 Hz, 1 H), 2.31−2.41 (m, 2 H), 2.02−2.23 (m, 3 H), 1.60−1.82 (m, 4 H), 1.21−1.59 (m, 6 H), 1.19 (d, J = 7.0 Hz, 3 H), 0.92−1.05 (m, 1 H), 0.88 (d, overlapped, 3 H), 0.87 (s, 9 H); ^{13}C NMR (75 MHz, $CDCl_3$) δ 176.4, 78.5, 40.1, 37.6, 36.2, 34.6, 34.4, 33.0, 29.7, 28.7, 26.3, 26.0, 23.0, 22.7, 20.7, 17.2; HRESIMS m/z 394.2558 $[M + Na]^+$ (calcd for $C_{20}H_{37}NO_5Na$, 394.2563).

*14-epi-Palmyrolide Alcohol (**12**).* Compound **12** was prepared in a similar manner to **9**. The crude product was purified via column chromatography (100% EtOAc) to afford compound **12** (0.004 g, 94%): $[\alpha]_D^{25.5}$ +30.8 (c 0.24, $CHCl_3$); IR (neat, thin film) ν 3304, 2950, 1729, 1649, 1560, 1462, 1366, 1163, 1074 cm^{-1}; ^{1}H NMR (300 MHz, $CDCl_3$) δ 6.25 (bs, 1 H), 4.76 (dd, J = 9.9, 1.6 Hz, 1 H), 3.55−3.70 (m, 2 H), 2.77 (d, J = 4.8 Hz, 3H), 2.37−2.50 (m, 1 H), 2.27 (bs, 1 H), 2.00−2.20 (m, 2 H), 1.63−1.83 (m, 2 H), 1.21−1.60 (m, 10 H), 1.16 (d, J = 7.0 Hz, 3 H), 0.92−1.04 (m, 1 H), 0.86 (d, overlapped, 3 H), 0.85 (s, 9H); ^{13}C NMR (75 MHz, $CDCl_3$) δ 177.0, 174.1, 78.4, 62.2, 40.0, 37.5, 36.2, 34.6, 34.5, 33.1, 32.4, 28.8, 26.1, 25.9, 23.6, 23.1, 20.7, 17.7; HRESIMS m/z 380.2764 $[M + Na]^+$ (calcd for $C_{20}H_{39}NO_4Na$, 380.2771).

Cerebrocortical Neuron Culture. Primary cultures of cerebrocortical neurons were obtained from embryonic day 17 Swiss-Webster mice as described elsewhere.[8] Briefly, pregnant mice were euthanized by CO_2 asphyxiation, and embryos were removed under sterile conditions. Cerebral cortices were collected, stripped of meninges, minced by trituration with a Pasteur pipet, and treated with trypsin for 25 min at 37 °C. The cells were then dissociated by two successive trituration and sedimentation steps in soybean trypsin inhibitor and DNase-containing isolation buffer, centrifuged, and resuspended in Eagle's minimal essential medium with Earle's salt (MEM) supplemented with 1 mM L-glutamine, 10% fetal bovine serum, 10% horse serum, 100 IU/mL penicillin, and 0.10 mg/mL streptomycin (pH 7.4). Cells were plated onto poly-L-lysine-coated 96-well (9 mm), clear-bottomed, black-well culture plates (MidSci) at a density of 1.5 × 10^5 cells/well. Cells were then incubated at 37 °C in a 5% CO_2 and 95% humidity atmosphere. The culture media was changed every other day, starting from day 5 *in vitro* using a serum-free growth medium containing Neurobasal medium supplemented with B-27, 100 IU/mL penicillin, 0.10 mg/mL streptomycin, and 0.2 mM L-glutamine. Neocortical cultures were used in experiments between 7 and 9 days *in vitro*. All animal use protocols were approved by the Institutional Animal Care and Use Committee (IACUC) of Creighton University.

Intracellular Sodium Concentration Measurement. $[Na^+]_i$ measurement and full *in situ* calibration of sodium-binding benzofuran isophthalate fluorescence ratio were performed as described previously.[3] Cells were grown in 96-well plates and washed four times with Locke's buffer (8.6 mM HEPES, 5.6 mM KCl, 154 mM NaCl, 5.6 mM glucose, 1.0 mM $MgCl_2$, 2.3 mM $CaCl_2$, 0.1 mM glycine, pH 7.4) using an automated microplate washer (BioTek Instruments). After measuring the background fluorescence of each well, cells were incubated for 1 h at 37 °C with dye-loading buffer (100 μL/well) containing 10 μM SBFI-AM (Invitrogen) and 0.02% Pluronic F-127 (Invitrogen). Cells were washed five times with Locke's buffer, leaving a final volume of 100 μL in each well. The plate was then transferred back to the incubator for 15 min to allow the cells to equilibrate after washing and placed in a FlexStation II (Molecular Devices) chamber to detect Na^+-bound SBFI emission at 505 nm (cells were excited at 340 and 380 nm). Fluorescence readings were taken once every 5 s for 60 s to establish the baseline, and then 50 μL of different concentrations of (−)-palmyrolide A and/or veratridine was added to each well from the compound plate at a rate of 26 μL/s, yielding a final volume of 200 μL/well. After correcting for background fluorescence, SBFI fluorescence ratios (340/380) and concentration−response graphs were generated using GraphPad Prism (GraphPad Software Inc.).

Compound Preparation for Intracellular Sodium Concentration Measurement. Each palmyrolide A analogue was dissolved in DMSO at a stock concentration of 50 mM and stored at −20 °C until used. On the day of an experiment, an aliquot of stock solution was diluted in Locke's buffer. This dilution in Locke's buffer resulted in palmyrolide A analogue solutions that were 4 times the desired final concentration.

NMR and Computational Methods. (−)-Palmyrolide A (**1**) and analogues (**2**, **7**, and **8**) were dissolved in $CDCl_3$ at a concentration of ~2.5 mg in 50 μL and transferred to a 1.7 mm NMR tube. Spectra were acquired at 298 K using standard Bruker NMR pulse sequences. The NOESY mixing time was 500 ms, the HMBC delay was set to 6.25 ms (8 Hz), and the HETLOC used a DISPI-2 spinlock of 60 ms duration. Chemical shift assignments were based on analysis of the DQF-COSY, HSQC, and HMBC 2D experiments using UCSF Sparky.[9] TopSpin (Bruker Biospin) was used to analyze coupling constants in the ^{1}H NMR and HETLOC spectra. NOESY peak heights were converted to upper distance restraints of 3, 4, 5, or 6 Å using in-house Perl scripts. Where restraints involved a group of atoms, pseudoatom corrections were applied by the Amber restraint generation tools. Initial atomic coordinates were prepared using Avogadro.[10] Force field parameters were estimated using the GAFF force field[11] and the antechamber program in the Amber 14 package.[12] Molecular dynamics simulations were nonperiodic, vacuum simulations with a distance-dependent dielectric term. Using Sander in the Amber 14 package each starting structure was energy minimized, then subjected to 20 ps of simulated annealing with the NMR-derived restraints in which the temperature was raised from 10 K to 600 K then cooled to near 0 K. The simulated annealing was run 20 times for each structure with a different random number seed each time. Each collection of 20 structures was sorted by restraint violation energy, and outliers were discarded. To align structures, the selected ensemble was superimposed on C1−7, O12, C13−18, and N19 using cpptraj.[13] To stereospecifically assign pairs of diastereotopic hydrogens, pairs of NOEs that involved the diastereotopic atoms and had differential intensities were identified, then compared with the distances between these atoms in the ensemble of selected structures. If the ensemble

mean of one distance was more than one standard deviation from the alternative, then the diastereotopic hydrogens were stereospecifically assigned. Structures were visualized with UCSF Chimera.[14]

■ ASSOCIATED CONTENT

Supporting Information

Copies of ^{1}H, ^{13}C, and multidimensional NMR spectra and tabulated data. Lists of restraints used in structure calculations. This material is available free of charge via the Internet at http://pubs.acs.org.

■ AUTHOR INFORMATION

Corresponding Author

*E-mail: wmaio@nmsu.edu. Phone: 575-646-4017. Fax: 575-646-2505.

Present Address

[‖]Department of Chemistry, New Mexico Institute of Mining and Technology, Socorro, New Mexico 87801, United States.

Author Contributions

[‡]S. Mehrotra and B. M. Duggan contributed equally.

Notes

The authors declare no competing financial interest.

■ ACKNOWLEDGMENTS

We would like to thank the NIH (2RO1NS0533398-11; W.H.G. and T.F.M.) and New Mexico State University (W.A.M.) for providing financial assistance in support of this work. W.A.M. would also like to thank Mr. B. Rose for helpful discussions.

■ REFERENCES

(1) Pereira, A. R.; Cao, Z.; Engene, N.; Soria-Mercado, I. E.; Murray, T. F.; Gerwick, W. H. *Org. Lett.* **2010**, *12*, 4490−4493.

(2) (a) Klein, D.; Braekman, J. C.; Daloze, D.; Hoffmann, L.; Demoulin, V. *Tetrahedron Lett.* **1996**, *37*, 7519−7520. (b) Klein, D.; Braekman, J. C.; Daloze, D.; Hoffmann, L.; Castillo, G.; Demoulin, V. *J. Nat. Prod.* **1999**, *62*, 934−936. (c) Matthew, S.; Salvador, L. A.; Schupp, P. J.; Paul, V. J.; Luesch, H. *J. Nat. Prod.* **2010**, *73*, 1544−1552.

(3) Luesch, H. L.; Yoshida, W. Y.; Moore, R. E.; Paul, V. J.; Corbett, T. H. *J. Am. Chem. Soc.* **2001**, *123*, 5418−5423.

(4) (a) Rahbaek, L.; Anthoni, U.; Chrisophersen, C.; Nielsen, P.; Petersen, B. *J. Org. Chem.* **1996**, *61*, 887−889. (b) Gournelis, D. C.; Laskaris, G. G.; Verpoorte, R. *Nat. Prod. Rep.* **1997**, *14*, 75−82. (c) Lin, H.-Y.; Chen, C.-H.; You, B.-J.; Liu, K. C. S. C.; Lee, S.-S. *J. Nat. Prod.* **2000**, *63*, 1338−1343. (d) Sergeyev, S. A.; Hesse, M. *Helv. Chim. Acta* **2003**, *86*, 465−473. (e) Carr, G.; Poulsen, M.; Klassen, J. L.; Hou, Y.; Wyche, T. P.; Bugni, T. S.; Currie, C. R.; Clardy, J. *Org. Lett.* **2012**, *14*, 2822−2825. See also ref 2.

(5) For several examples, see: (a) Palermo, J. A.; Rodriguez, M. F.; Seldes, A. M. *Tetrahedron* **1996**, *52*, 2727−2734. (b) Erickson, K. L.; Beutler, J. A.; Cardellina, J. H., II; Boyd, M. R. *J. Org. Chem.* **1997**, *62*, 8188−8192. (c) Galinis, D. L.; McKee, T. C.; Pannell, L. K.; Cardellina, J. H., II; Boyd, M. R. *J. Org. Chem.* **1997**, *62*, 8968−8969. (d) McKee, T. C.; Galinis, D. L.; Pannell, L. K.; Cardellina, J. H., II; Laakso, J.; Ireland, C. M.; Murray, L.; Capon, R. J.; Boyd, M. R. *J. Org. Chem.* **1998**, *63*, 7805−7810. (e) Kim, J. W.; Shin-ya, K.; Furihata, K.; Hayakawa, Y.; Seto, H. *J. Org. Chem.* **1999**, *64*, 153−155. (f) Kohno, J.; Koguchi, Y.; Nishio, M.; Nakao, K.; Kuroda, M.; Shimizu, R.; Ohnuki, T.; Komatsubara, S. *J. Org. Chem.* **2000**, *65*, 990−995. (g) Bokesch, H. R.; Pannell, L. K.; McKee, T. C.; Boyd, M. R. *Tetrahedron Lett.* **2000**, *41*, 6305−6308. (h) Nogle, L. M.; Gerwick, W. H. *Org. Lett.* **2002**, *4*, 1095−1098. (i) Murcia, C.; Coello, L.; Fernández, R.; Martín, M. J.; Reyes, F.; Francesch, A.; Munt, S.; Cuevas, C. *Mar. Drugs* **2014**, *12*, 1116−1130.

(6) (a) Tello-Aburto, R.; Johnson, E. M.; Valdez, C. K.; Maio, W. A. *Org. Lett.* **2012**, *14*, 2150−2153. (b) Tello-Aburto, R.; Newar, T. D.; Maio, W. A. *J. Org. Chem.* **2012**, *77*, 6271−6289.

(7) (a) Wadsworth, A. D.; Furkert, D. P.; Sperry, J.; Brimble, M. A. *Org. Lett.* **2012**, *14*, 5374−5377. (b) Philkhana, S. C.; Seetharamsingh, B.; Dangat, Y. B.; Vanka, K.; Reddy, D. S. *Chem. Commun.* **2013**, *49*, 3342−3344. (c) Sudhakar, G.; Reddy, K. J.; Nanubolu, J. B. *Tetrahedron* **2013**, *69*, 2419−2429.

(8) (a) Cao, Z.; George, J.; Gerwick, W. H.; Baden, D. G.; Rainier, J. D.; Murray, T. F. *J. Pharm. Exp. Ther.* **2008**, *326*, 604−613. (b) Jabba, S. V.; Prakash, A.; Dravid, S. M.; Gerwick, W. H.; Murray, T. F. *J. Pharm. Exp. Ther.* **2010**, *332*, 698−709.

(9) UCSF Sparky: Goddard, T. D.; Kneller, D. G. *SPARKY 3*; University of California, San Francisco, CA.

(10) Hanwell, M. D.; Curtis, D. E.; Lonie, D. C.; Vandermeersch, T.; Zurek, E.; Hutchison, G. R. *J. Cheminf.* **2012**, *4*, 17.

(11) Wang, J.; Wolf, R. M.; Caldwell, J. W.; Kollman, P. A.; Case, D. A. *J. Comput. Chem.* **2004**, *25*, 1157−1174.

(12) Case, D. A.; Cheatham, T.; Darden, T.; Gohlke, H.; Luo, R.; Merz, K. M., Jr.; Onufriev, A.; Simmerling, C.; Wang, B.; Woods, R. *J. Comput. Chem.* **2005**, *26*, 1668−1688.

(13) Roe, D. R.; Cheatham, T. E., III *J. Chem. Theory Comput.* **2013**, *9*, 3084−3095.

(14) UCSF Chimera−a visualization system for exploratory research and analysis: Pettersen, E. F.; Goddard, T. D.; Huang, C. C.; Couch, G. S.; Greenblatt, D. M.; Meng, E. C.; Ferrin, T. E. *J. Comput. Chem.* **2004**, *25*, 1605−1612.